

Introduction

This study was motivated by the desire to further understand the pediatric ovary across an important early reproductive transition, puberty. Previous work has focused primarily on fetal-neonatal or perimenopausal transitions, leaving a gap in our understanding of the structural development accompanying hormonal and phenotypic changes that define puberty. Recent work uncovered the research potential of tissue derived from **ovarian tissue cryopreservation (OTC)** to answer fundamental questions in ovarian biology, especially with respect to the understudied pediatric population. In OTC, a patient undergoes unilateral oophorectomy to isolate and cryopreserve the superficial 1-2mm of ovarian tissue (cortex) containing dormant **primordial follicles (PMFs)**. This tissue will be used for future autologous re-transplantation upon loss of ovarian function and desire for conception and/or hormone restoration.

Purpose

The **purpose** of this work was to utilize specimens derived from OTC to describe **gross morphologic changes** in isolated ovaries and **identify sub-anatomical features that distinguish pre-pubertal and post-pubertal ovaries at the histologic level** using the ovarian surface epithelium as a consistent reference point. In doing so, this work provides added context for current and future studies that use this tissue and contributes to the overall body of work describing human ovarian development.

Methods

Human ovarian tissue collection. Pre-pubertal and post-pubertal samples were prospectively collected from 77 participants (53 pre-pubertal, 24 post-pubertal) undergoing ovarian tissue cryopreservation (OTC) for fertility preservation between 2018 and 2021. Pre-pubertal participants were defined as individuals displaying no physical signs of pubertal development (Tanner 1), and post-pubertal participants were defined as Tanner 2-5. At oophorectomy, a 3-4 mm biopsy is taken for routine pathology and evaluated by Lurie Children's Hospital (LCH) pathologists. Participants whose tissue was found to contain evidence of malignancy was excluded from this study.

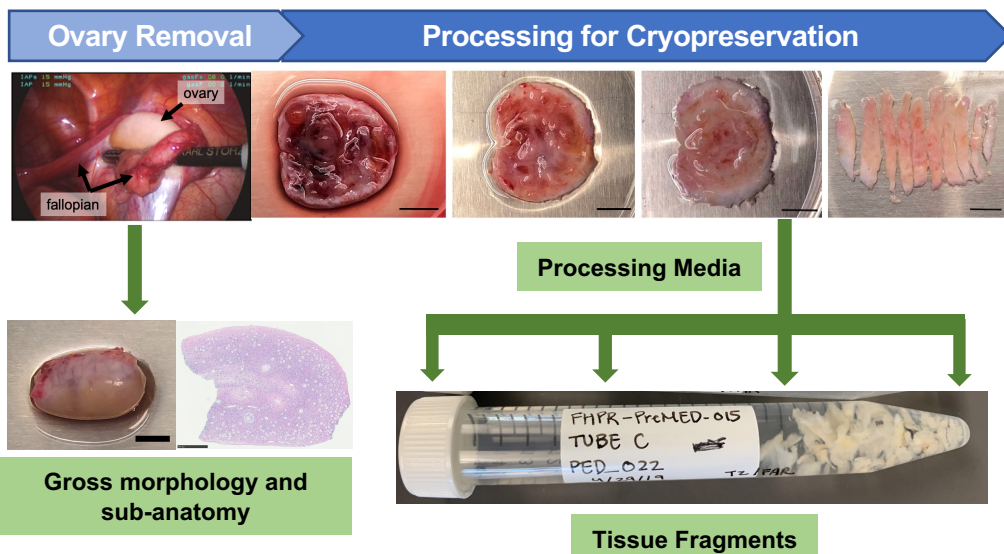


Figure 1. Experimental Workflow. Ovarian tissue removed laparoscopically for OTC was photographed and weighed prior to OTC processing. Length was measured across the long axis, and width was measured across the short axis, respectively. A single 3-4 mm biopsy of ovarian tissue obtained at oophorectomy was fixed, processed for histology, sectioned, and stained with hematoxylin and eosin for sub-anatomy analysis. Tissue fragments discarded in the processing media during OTC processing were collected and sorted into **RAN** (selected at random) and **FOL** (fragments identified to contain ovarian follicles by light microscopy) groups and were processed for histology, sectioned, and stained with hematoxylin and eosin for follicle counts.

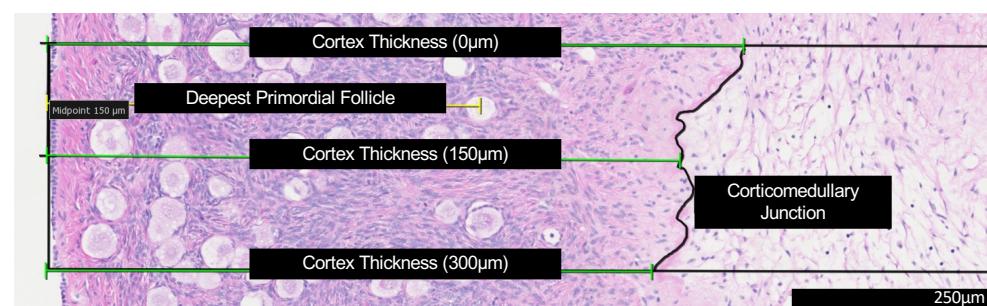


Figure 2. Sub-anatomy analysis. Sections were analyzed for: corticomedullary demarcation. If present, depth of cortex; depth of deepest PMF; follicle number and developmental stage per tissue area, and tunica albuginea. If present, depth of tunica albuginea was also recorded. All depths were measured relative to ovarian surface epithelium (OSE).

Results

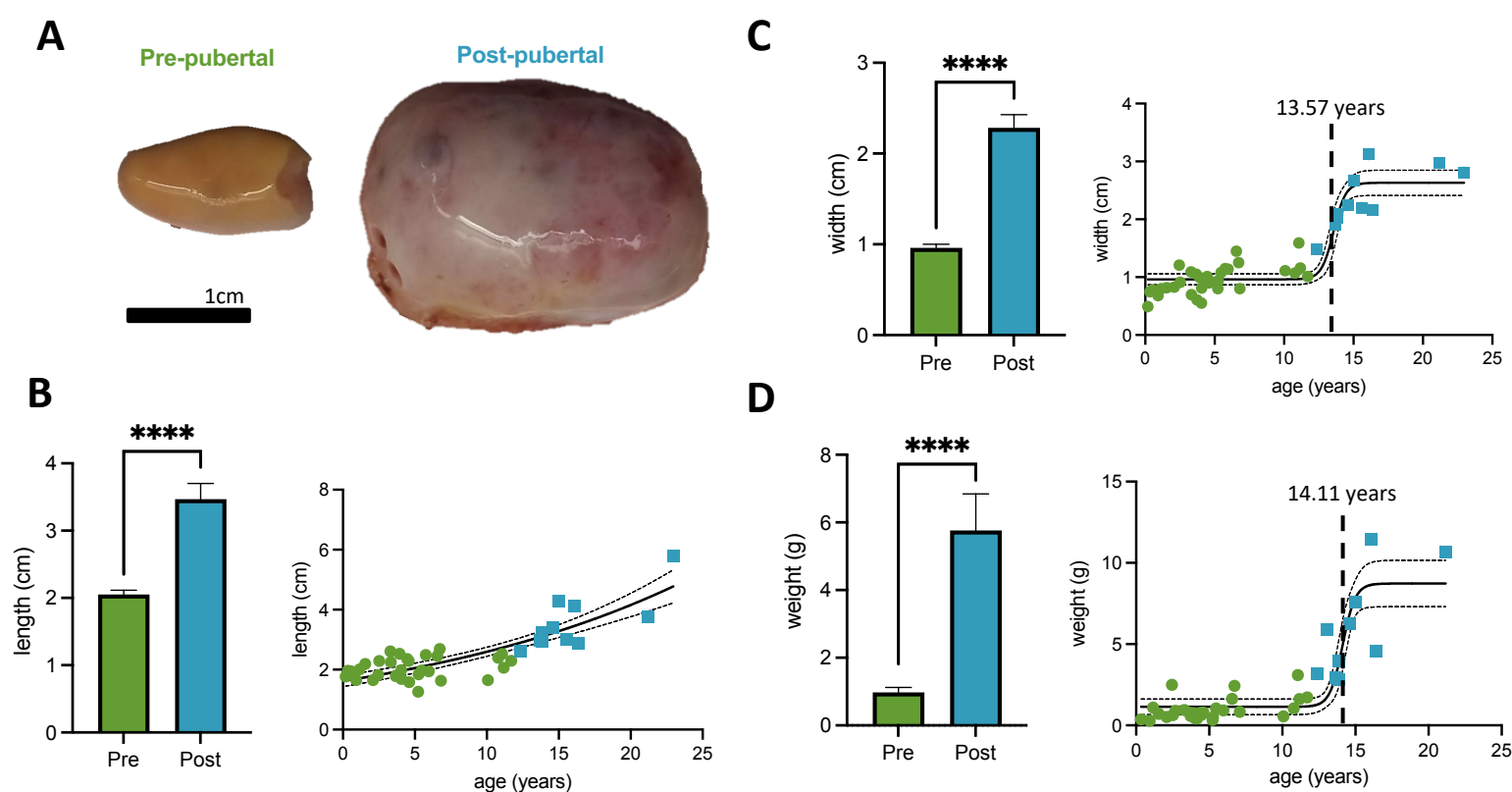


Figure 3. Gross morphologic analysis. A. Representative images of isolated pre-pubertal (4.6 years old) and post-pubertal (16.4 years old) ovaries prior to ovarian tissue cryopreservation. Morphometric analysis of isolated ovaries on average by puberty status and plotted by age for (B) length ($y = 1.599(e^{0.04823 \cdot Age})$, $R^2 = 0.71$), (C) width ($y = 0.9627 + \frac{1.6683}{1 + 10^{13.57 - Age}}$, $R^2 = 0.86$), and (D) weight ($y = 1.139 + \frac{7.591}{1 + 10^{14.11 - Age}}$, $R^2 = 0.77$), respectively. Solid line is equation of the line of best fit, dashed lines show 95% confidence interval.

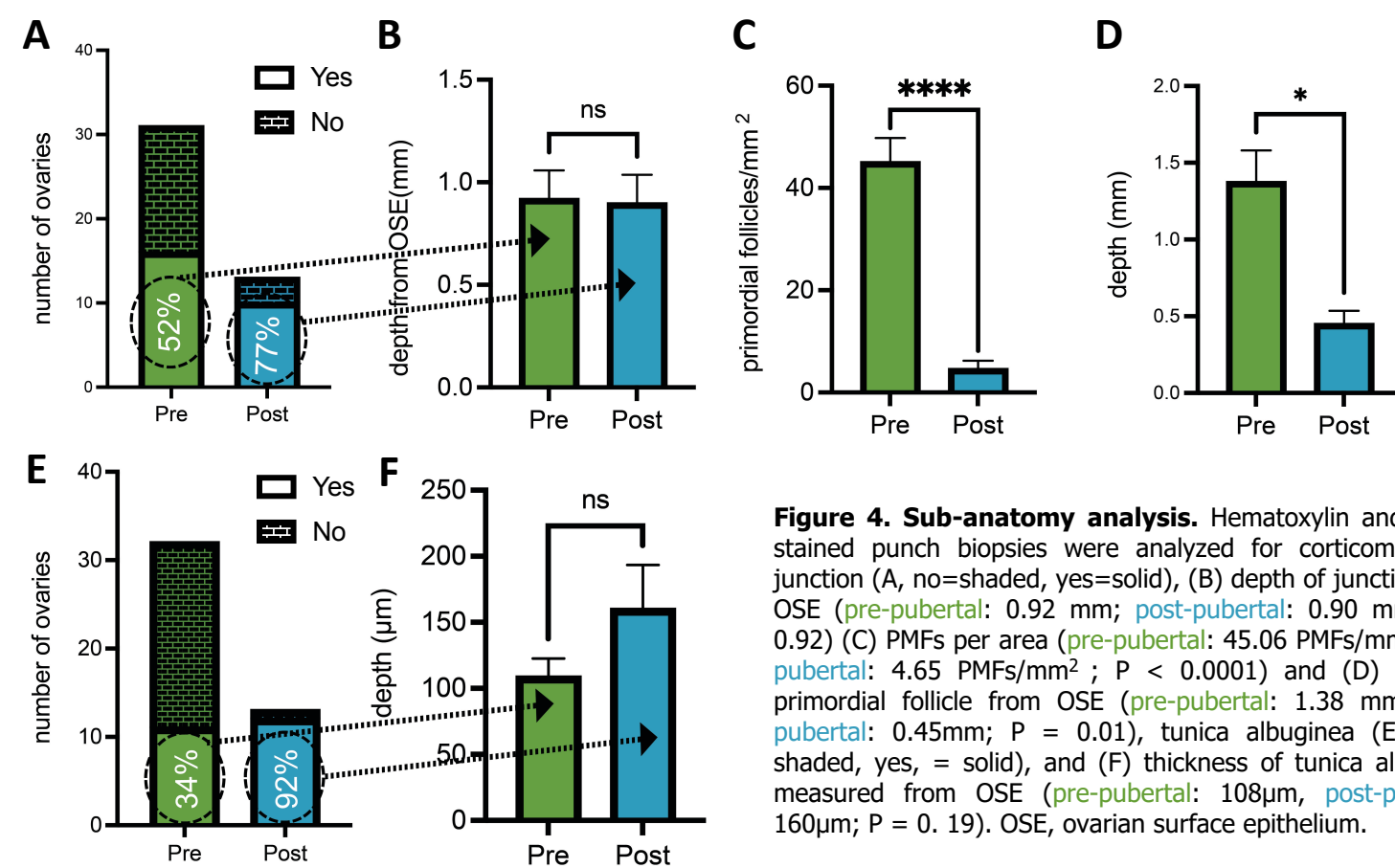


Figure 4. Sub-anatomy analysis. Hematoxylin and eosin-stained punch biopsies were analyzed for corticomedullary junction (A, no=shaded, yes=solid), (B) depth of junction from OSE (pre-pubertal: 0.92 mm; post-pubertal: 0.90 mm; $P = 0.92$) (C) PMFs per area (pre-pubertal: 45.06 PMFs/mm²; post-pubertal: 4.65 PMFs/mm²; $P < 0.0001$) and (D) deepest primordial follicle from OSE (pre-pubertal: 1.38 mm, post-pubertal: 0.45mm; $P = 0.01$), tunica albuginea (E, no = shaded, yes = solid), and (F) thickness of tunica albuginea measured from OSE (pre-pubertal: 108µm, post-pubertal: 160µm; $P = 0.19$). OSE, ovarian surface epithelium.

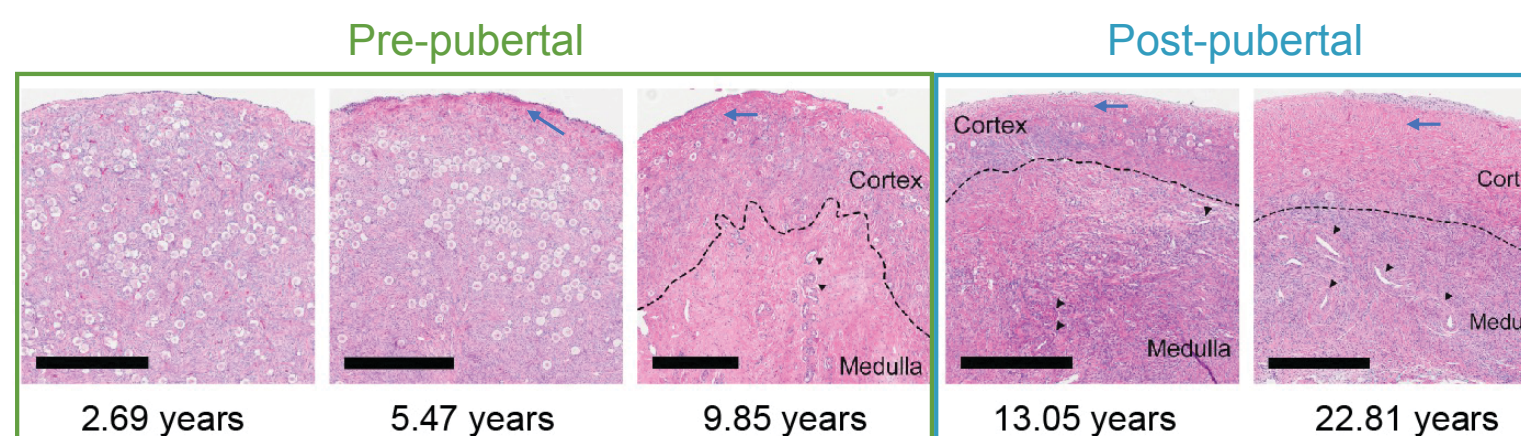


Figure 4. Sub-anatomy changes cross the pubertal transition. Representative punch biopsies spanning pubertal transition. Blue arrows denote tunica albuginea. Black arrowheads denote blood vessels. Scale, 500µm.

Results (cont.)

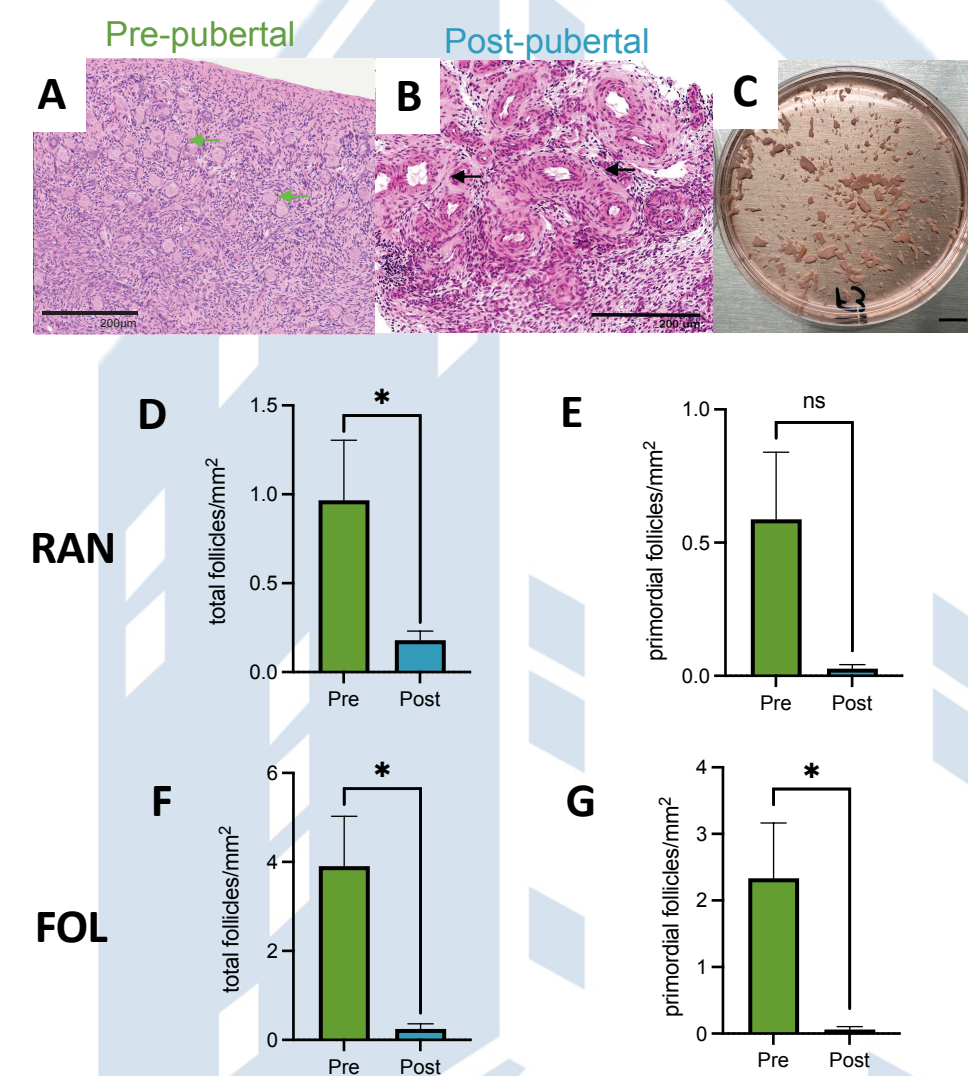


Figure 5. Follicle counts in tissue fragments. Representative images of sectioned and H&E-stained tissue fragments used for follicle counting, (A) pre-pubertal and (B) post-pubertal. Green arrowheads, PMFs. Black arrowheads, vessels. Scale, 200µm. (C) Fresh tissue fragments from the processing of pediatric ovaries for OTC in holding media. Quantitative analysis of total follicle density and PMF density for (D, E) RAN (total follicle density, $P = 0.05$; PMF density, $P = 0.0566$) and (F, G) FOL fragments (total follicle density, $P = 0.01$; PMF density, $P = 0.04$).

Discussion and Conclusions

- Width and weight of the ovary remains static during pre-puberty but rises rapidly following the pubertal transition to its post-pubertal plateau
- Sub-anatomic pubertal development is characterized by:
 - completion of compartmentalization
 - complete development of the tunica albuginea
 - reduced abundance of primordial and total follicles in the cortical region
 - superficial primordial follicles
- Standard pathology, metrics gathered during tissue processing, and tissue that would normally be discarded during OTC processing can be used for basic research regarding important aspects of pediatric biology that are not yet well understood.

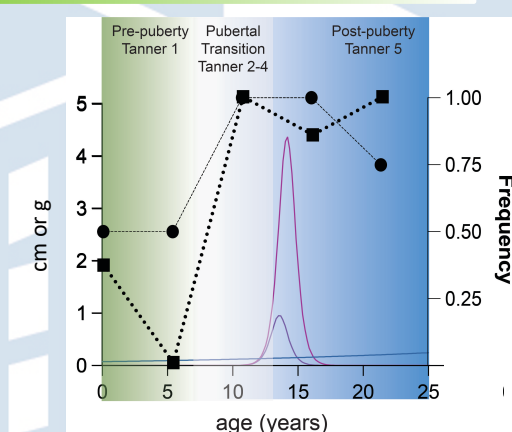


Figure 6. Timeline of ovarian development. Length (blue solid line). Width (purple solid line). Weight (pink solid line). Corticomedullary junction (circle and small dotted line). Tunica albuginea presence (square and large dotted line).

Acknowledgements

This work was supported in part by the Children's Research Fund, the Ann & Robert H. Lurie Children's Hospital Faculty Practice Plan award (MML), the Warren and Eloise Batts endowment, the Burroughs Wellcome Fund Career Award at the Scientific Interface (1014568, MML), the Eunice Kennedy Shriver National Institute of Child Health and Human Development, and the National Institutes of Health (R01HD104683, MML). ET was supported in part by NIH/NCI training grant T32 CA009560. The authors thank the generous supporters of FHRP research, Suzanne & Michael Burns, Mary and Ralph Gesualdo Family Foundation, and the Debicki Foundation. Histology services for this work were provided by the Northwestern University Pathology Core Facility, a Cancer Center Support Grant (NCI CA060553) and the Microscopy and Histology Group at Stanley Manne Children's Research Institute, affiliated with Ann & Robert H. Lurie Children's Hospital of Chicago.

The authors thank Grace Schwartz and Luhan (Tracy) Zhou for their assistance in OTC processing.

Contact information



elizabeth.tsui@northwestern.edu
Lab Website: larondalab.org
FHRP Website: https://tinyurl.com/3wru944r